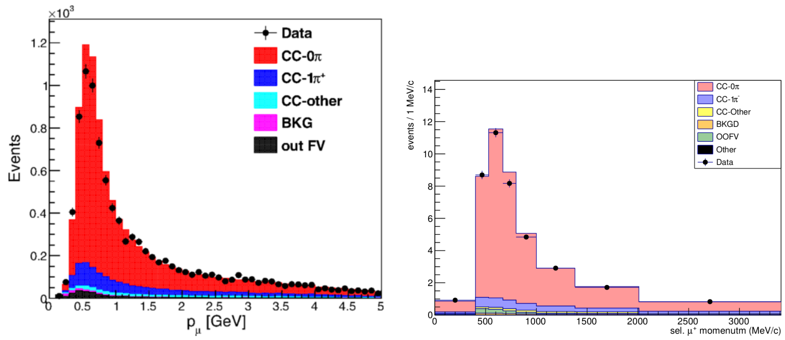


**(a)** CC $0\pi$ Selection [**?**] **(b)** CC $0\pi$ Selection [**?**]

**Figure 1:** Data and MC distributions of the () water-in and CC $0\pi$ signal selections. They importantly share the same pre-selection cuts as this analysis. The plots have been normalized to data POT and are sorted into various truth topologies.

This section describes the development of and CC Inclusive selections in both FHC and RHC beam configuration for ()-based analyses. These selections are the continuation of previous works that developed CC Inclusive selections between the () and the TPC. The first such analysis was the CC Inclusive cross-section using the previous ND280 simulation and reconstruction software called Production 5 [**?**]. That analysis relied on each sub-detector's reconstruction software and developed a track matching algorithm since the ND280 "Global" reconstruction matching was not available in that software production. Another cross section analysis measuring the cross section ratio of / also used this "pre-Global" technique with the modern T2K Production 6 software [**?**]. As the inter-detector matching reconstruction became available in Global, two cross section analyzes, CC $0\pi$ [**?**] and CC $0\pi$ [**?**, **?**], were developed that also used the CC Inclusive selection as pre-selection cuts. These pre-selection cuts are well validated and have published results as shown in Figure 1 on page 1.The selections described in this thesis also employ the same pre-selection cuts with the latest stable Global reconstruction software, Production 6. What follows from here in this section is a layout of the following topics.

The first topic is the event reconstruction using the "Global" reconstruction software. Next is the pre-selection cut flow. With the pre-selection cuts established, each of the three CC Inclusive selection's cut flow is described. Concluding this section is a discussion of the three samples in the following order: in FHC mode, in RHC, and background in RHC.

## 0.1 Global Reconstruction

The task of the Global reconstruction is to combine all the ND280 information into a combined reconstructed object. It was originally designed to analyze "CCQE-like" events in the Tracker, FGD+TPC, region and has been extended to operate with all of ND280. A brief description of the Global reconstruction is described below.

The Global reconstruction is a software package that attempts to recognize patterns of data to form tracks and find vertices for those tracks. Particle shower reconstruction in Global will not be discussed in this thesis since no shower objects are considered. Each sub-detector reconstruction is run as the seed to Global's track matching algorithms. This includes the ()'s track-finding algorithms, which defines a () track as a sequence of nodes each at a single bar layer. To facilitate inter-detector matching, Global attempts to re-fit the () track using a Kalman filter. The re-fit procedure also corrects for particle energy loss as a function of length ($dT/dx$) and multiple scattering processes. A () vertex, which is the reconstructed location of the neutrino interaction, is then associated with the re-fit track using another Kalman filter algorithm. Matching tracks between the () and the TPC is done automatically in the ND280 Global fit.

## 0.2 () Selection Cuts

The selection of CC Inclusive events use a series of cuts to select the primary lepton. The pre-selection cuts ("precuts") are applied first to extract events that start in the () FV. A minimum ionizing particle (MIP) is more likely to reach TPC1 from the () fiducial volume (FV) since the () is constructed out of heavy materials especially in the CECal. So the main track each selection is designed to select a muon.

This following sections will describe the precuts common to all CC Inclusive selections and the branching of different cuts, after the precuts, to select the main track.

### 0.2.1 Precuts

The precuts were initially developed to select CC Inclusive using the () and TPC sub-detector reconstruction softwares separately [**?**, **?**]. They were then used with the Global reconstruction software for the selection in the FHC beam configuration [**?**]. The description and sequence of the precuts is described below.

The following precuts are checked on the collected data from each Trip-T integration cycle as follows:

1. The event has a "good" data quality flag.
   - An event is rejected if any sub-detector or electronics in ND280 reported as "bad" during that bunch.
2. There is at least one (1) track reconstructed in TPC1.
   - There are no restrictions on the number of tracks fully contained in the () or exiting into other sub-detectors.
3. The track in TPC1 must have more than 18 nodes.
   - The TPC reconstruction gathers vertical and horizontal hits into clusters of hits. The charge distribution of the cluster is used to get a vertical (horizontal) position that is more accurate than the individual readout pads. A node is constructed out of each cluster with associated track state information. The set of nodes are used to fit the track into a "helix" [**?**].
4. The reconstructed vertex is within the () WT FV.
   - The () FV is defined to include as much as the WT regions as possible. Its X and Y borders are 25 cm away from the ()ule edges while its Z borders intersect the last and first half downstream ()ule in the USECal and CECal, respectively. The enumerated volume edges are shown in Table 1 on page 4. This volume, while used for track-based analyzes in the past, was optimized for and analyzes.

5. All tracks that enter TPC1 pass the veto cut

   - An event is rejected if any () track enters TPC1 from outside the "corridor" volume. This cut was designed to eliminate broken tracks between the () and TPC1 the pre-Global separate sub-detector reconstruction was used. [**?**]. In practice, this cut ensures that Global tracks entering TPC1 away from its X and Y edges. The corridor definition is the same as defined in T2K-TN-208 and shown in Table 1 on page 4.

| () WT FV | | | Corridor Volume | | |
|---|---|---|---|---|---|
| -836 | < X < | 764 | -988 | < X < | 910 |
| -871 | < Y < | 869 | -1020 | < Y < | 1010 |
| -2969 | < Z < | 1264 | -3139 | < Z < | -900 |

**Table 1:** The () WT FV (left) and veto corridor volume (right) in the ND280 coordinate system. The corridor spans from the 5th (8th) to 40th (80th) ()ule (scintillator layer). All the units are given in millimeters.

After passing all the precuts, a single, global track, which is observed in TPC1, is assigned as the lepton candidate or "main track" of a selection.

The momentum of the main track, $P$, is sum of its momentum in the TPC, $P_{\text{TPC}}$, with the estimate momentum lost in the (), $\Delta P$

$P = P_{\text{TPC}} + \Delta P$

. (1)

Momentum lost in the () is estimated by first summing the total energy loss, $\Delta T$, along the track path $\mathcal{C}$

$$\Delta T = \int_{\mathcal{C}} \left( \frac{dT}{dx} \right) dx. \tag{2}$$

Using the chain rule, we can convert the energy loss function, $dT/dx$, into momentum loss

$$
\begin{aligned}
\frac{dT}{dx} &= \left(\frac{dT}{dP}\right)\left(\frac{dP}{dx}\right) \\
&= \left(\frac{Pc^2}{E}\right)\left(\frac{dP}{dx}\right) \\
&= \beta c \left(\frac{dP}{dx}\right),
\end{aligned} \tag{3}
$$

where $\beta$ is the changing particle velocity as a ratio of the speed of light $c$. The fundamental theorem of Calculus permits the us to write the energy loss as a momentum loss along the track's path $\mathcal{C}$ as

$$\Delta P$$

$=\int_{\mathcal{C}} \left(\frac{dP}{dx}\right) dx = \frac{1}{c}\int_{\mathcal{C}} \left[\left(\frac{dT}{dx}\right)\frac{1}{\beta(x)}\right] dx.$(4)Since the reconstructed track's path $\mathcal{C}$ is not infinitesimally precise due to inherent detector resolution, we must replace the integral with a sum and differential $dx \rightarrow \Delta x$. We then arrive at the expres7sion of the momentum loss estimate in the () as

$$P = P_{\text{TPC}} + \frac{1}{c}\sum_{t}\left[\left(\frac{dT}{dx}\right)\left(\frac{\Delta x}{\beta(x)}\right)\right]_t. \tag{5}$$

For most tracks entering the TPC, they will be highly relativistic in the () ($\beta \approx 1$), and (5) simplifies to

$$P = P_{\text{TPC}} + \frac{1}{c}\sum_{t}\left[\left(\frac{dT}{dx}\right)\Delta x\right]_t \tag{6}$$

The next sections describe the selection cuts, first in FHC mode and then RHC mode.

### 0.2.2 CC Inclusive in FHC Cut

- The highest momentum negatively charged track (HMNT) is the lepton candidate

As discussed in Section 0.2.1 on page 3, this selection is the basis for the analysis. In FHC mode, the vast majority of neutrino interactions are CC events producing an outgoing, negatively charged muon. So if there is no negatively charged track in the TPC, the event is rejected.

### 0.2.3 CC Inclusive in RHC Cuts

- The highest momentum positively charged track (HMPT) is the lepton candidate
- The HMPT must be the highest momentum track (HMT)

In RHC, the majority of neutrinos in the beam is  since the horn focuses negatively charged pions. To select  CC interaction events by selecting positively charged muons, the lepton candidate is the HMPT in the TPC. The event is rejected if there is no positively charged track. However, since the RHC mode beam is not as  pure as the FHC beam, another cut was added to reduce this effect.

Since RHC neutrino beam can be described as a -enhanced beam, the HMPT must also be the HMT due to the significant "wrong-sign"  background. This effect is two fold due to the nature of the neutrino source and the cross section between neutrinos and antineutrinos. Firstly the neutrino flux is larger in RHC mode due to neutrino production at the target. The source of neutrinos are from mainly positively charged pions and kaons decays produced proton collisions on a graphite target. This method is more likely to produce positively charged pions in the target than negatively charged one. While the horns are designed to select the negatively charged pions in RHC mode, the excess amount of positively charged pions will penetrate the horn's filter. Therefore there are many more $\rightarrow +$ decays in RHC compared to FHC mode. Secondly, antineutrino interactions on matter are suppressed compared to neutrinos due to helicity considerations as explained in **??** on page ??.

### 0.2.4 Background CC Inclusive in RHC Cuts

- The highest momentum negative track (HMNT) is the lepton candidate
- The HMNT must be the highest momentum track (HMT)

As discussed in 0.2.3, the RHC neutrino beam has a significant wrong-sign  background. The selection of the HMNT is designed to select the negatively charged muons. To prevent selecting the antineutrino events, the HMNT must also be the HMT. The event is rejected if there is no negatively charged track. If there are both positively and negatively charged tracks, the HMT cut discriminates if the event originates from a  or .

## 0.3 Selection Kinematics

This section examines the kinematics for each of selections while differentiating between water-in and water-out mode. The selection cuts were implemented in Psyche which is the software interface that BANFF uses to select events. The data sets used in this analysis are runs 2-8 in both  () water-in and water-out (air) modes as shown in Table 2 on page 8. There will be no data events shown to prevent any potential biases that exist between the data and MC. Simulated events will be broken down into various true categories to understand selection kinematics, efficiencies, and purities.

The legends used are blown up , , and Figure 4 on page 11.

True interactions for these selections are generally divided into four interactions classes as shown in Figure 3 on page 11: neutrino CCQE ($\nu$ CCQE), neutrino non-CCQE ($\nu$ non-CCQE), antineutrino CCQE ($\overline{\nu}$ CCQE), and antineutrino non-CCQE ($\overline{\nu}$ non-CCQE). A $\nu$ CCQE interaction corresponds to a true NEUT generated  and  CCQE event at the interaction vertex. The  CCQE interaction corresponds to a true NEUT generated  and  CCQE event at the interaction vertex. The $\nu$ non-CCQE events are all $\nu$ interactions but $\nu$ CCQE. And finally the  non-CCQE events are all other  interactions but  CCQE. The non-CCQE definition somewhat awkward given the NC interaction is flavor agnostic, but the NEUT interaction generator differentiates between $\nu$ and  NC events.

The non-CCQE category is divided among the dominant T2K CC and all NC interactions modes as shown in Figure 2 on page 10. The “2p2h” [**?**] category refers to the CC interaction mode where a neutrino scatters off neighboring and interacting nucleon pairs. The CC-1$\pi$ category is a neutrino-induced resonance state that decays into a single pion. The CC-N$\pi$ state

| Run Period | Horn Current | () Status | Data POT $(\times 10^{20})$ | MC POT $(\times 10^{20})$ |
|---|---|---|---|---|
| 2 | +250 kA | Water | 0.4339 | 12.03 |
| | | Air | 0.3591 | 9.239 |
| 3b | +205 kA | | 0.2172 | 4.478 |
| 3c | +250 kA | | 1.364 | 26.32 |
| 4 | | | 1.782 | 34.99 |
| | | Water | 1.642 | 34.97 |
| 5c | -250 kA | | 0.4346 | 22.77 |
| 6b | | Air | 1.288 | 14.17 |
| 6c | | | 0.5058 | 5.275 |
| 6d | | | 0.7753 | 6.884 |
| 6e | | | 0.8479 | 8.594 |
| 7b | | Water | 2.436 | 33.70 |
| 8 | +250 kA | | 1.580 | 26.46 |
| | | Air | 4.148 | 36.06 |
| Sand | FHC | | - | 11.19 |
| Sand | RHC | | - | 12.92 |
| 2, 3b, 3c, 4, 8 | FHC | Air | 7.872 | 79.18 |
| 2, 4, 8 | | Water | 3.657 | 73.47 |
| 6b, 6c, 6d, 6e | RHC | Air | 3.417 | 34.92 |
| 5c, 7b | | Water | 2.871 | 56.48 |

**Table 2:** T2K MC and data POT divided by run periods. The bottom four rows are the aggregrated periods grouped by horn current and () status which is how the data analysis is performed.

| Categories | | NEUT Code |
|---|---|---|
| CCQE | CCQE | $-1$ |
| non-CCQE | 2p2h | $-2$ |
| | CC-1$\pi$ | $-16 \rightarrow -11$ |
| | CC-N$\pi$ | $-21$ |
| | CC-DIS | $-26$ |
| | CC-Other | $-17, -22, -23$ |
| | NC | $-100 \rightarrow -31$ |

**(a)** Antineutrino NEUT reactions

| $\nu$ Categories | | NEUT Code |
|---|---|---|
| $\nu$ CCQE | $\nu$ CCQE | $1$ |
| $\nu$ non-CCQE | $\nu$ 2p2h | $2$ |
| | $\nu$ CC-1$\pi$ | $11 \rightarrow 16$ |
| | $\nu$ CC-N$\pi$ | $21$ |
| | $\nu$ CC-DIS | $26$ |
| | $\nu$ CC-Other | $17, 22, 23$ |
| | $\nu$ NC | $31 \rightarrow 100$ |

**(b)** Neutrino NEUT reactions

**Table 3:** Table of NEUT reactions by name and number.

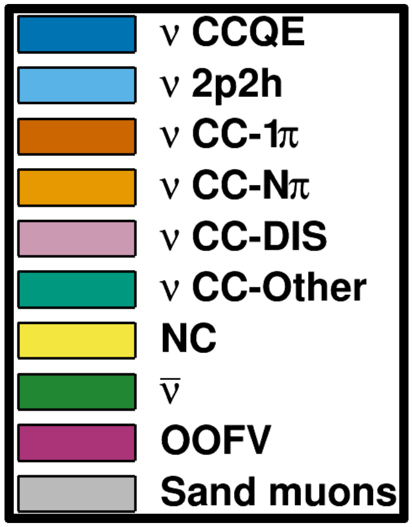


**Figure 2:** The enlarged NEUT interaction legend used in this section.

### 0.3.1 in FHC CC 1-Track

This selection provides the CCQE-like samples in FHC mode. Figure 5 on page 12 displays the momentum and angular distributions that are inputs to BANFF.

In the majority of cases, the lepton candidate is the true muon, making this a very pure sample. We can examine the efficiencies and purities differentially for true CCQE interactions in Figure 6 on page 13 A careful distinction must be made here for interactions that are $\nu$ CC but not . The efficiency, $\epsilon$, and purity, $\rho$, are defined as

$$\epsilon = \frac{N^{\text{True}}_{\text{Selected}}}{N^{\text{True}}} \qquad \rho = \frac{N^{\text{True}}_{\text{Selected}}}{N_{\text{Selected}}}, \tag{7}$$

where $N^{\text{True}}_{\text{Selected}}$ is the number of true, selected events, $N^{\text{True}}$ is the number of true events, and $N_{\text{Selected}}$ is the number of selected events. They demonstrate that the purity is highest near $0.5$ GeV/c with the efficiency highly dependent on the track angle.

The underlying true kinematics, $E_\nu$ and $Q^2$, of the interactions are shown in Figure 7 on page 13 which are of theoretical importance in the cross section and flux models. An interesting CCQE-like topology in this selection are “2 particle 2 hole” (2p2h) [**?**] events where neutrino scatters off a correlated neighboring and interacting nucleon pairs. Interaction model for 2p2h are included the

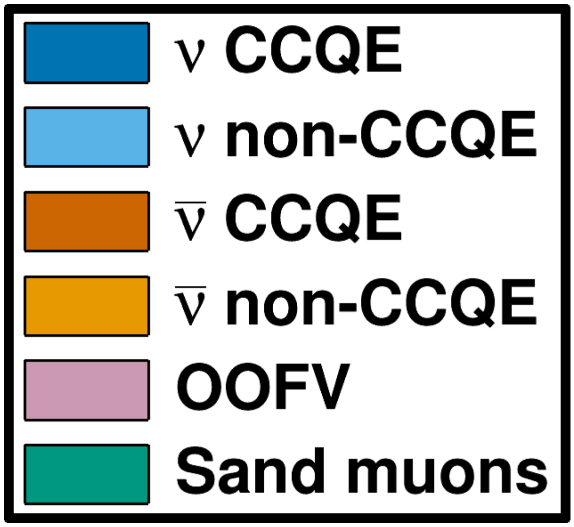


**Figure 3:** The NEUT CCQE and non-CCQE legend

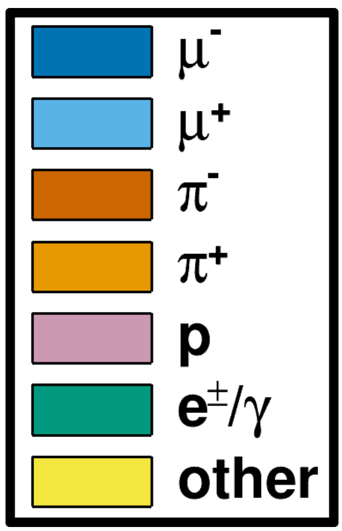


**Figure 4:** True particle selected legend

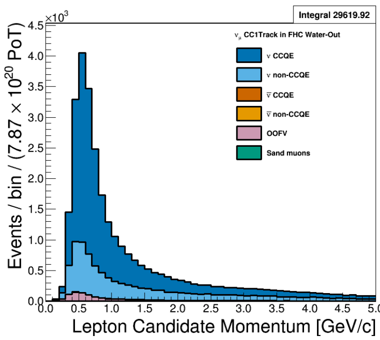


**(a)** Water-out

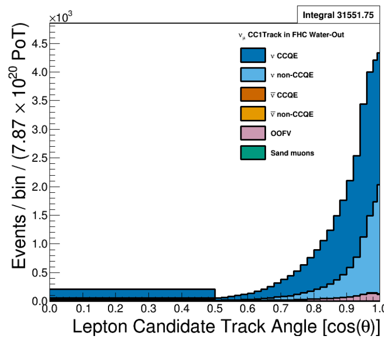


**(b)** Water-out

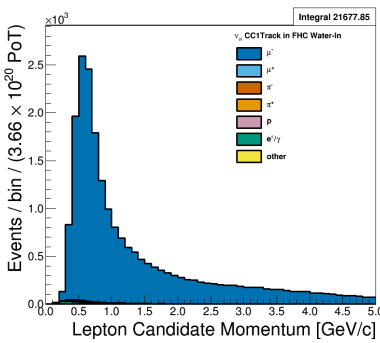


**(c)** Water-in

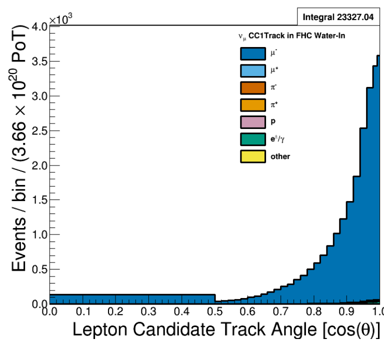


**(d)** Water-in

**Figure 5:** Lepton candidate reconstructed $P$ and $\cos\theta$ distributions for the  in FHC CC 1-Track selection. The top figures, (a) and (b), are displaying the true neutrino interaction at the vertex and normalized to the FHC water-out mode POT. The bottom figures, (c) and (d), are displaying the true particle selected and POT normalized for the FHC water-in mode POT.

BANFF fit whose model uncertainties are quite large in T2K. Therefore these events could reduce the 2p2h model uncertainties.

This selection contains a modest fraction of non-CCQE interactions. The largest contamination is $1$ interactions, which can happen primarily for a couple of reasons. Firstly, when the final state pion is produced, it is subject to final state interactions (FSI) where a pion can be absorbed or scattered in the nucleus. Secondly, and more importantly, a pion might not be reconstructed as a track in the  () if its energy is below reconstruction threshold. Together, the large $1$ background affects the CC $0\pi$ and CC $1\pi$ model parameters in the BANFF fit.

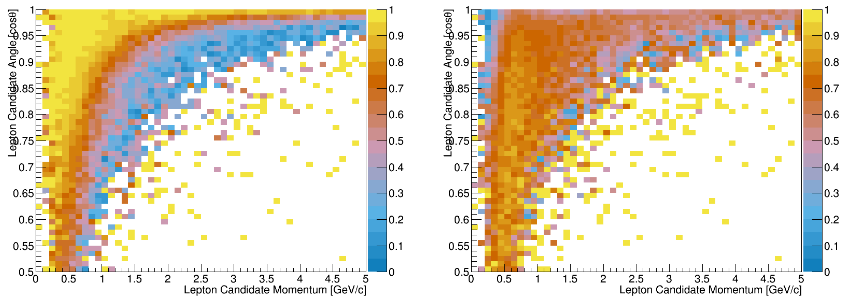


**(a)** True CCQE Efficiency **(b)** True CCQE Purity

**Figure 6:** The efficiency and purity of CCQE interactions in the  in FHC CC 1-Track selection. True events are defined as correctly matched  tracks from -induced CCQE interactions at the vertex .

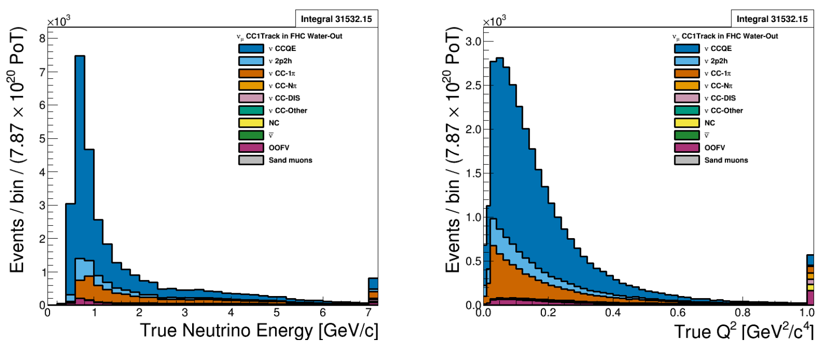


**(a)** Neutrino Energy **(b)** True $Q^2$

**Figure 7:** The  in FHC CC 1-Track true $E_\nu$ and $Q^2$ kinematics broken down by true NEUT interaction modes. Water-out mode is displayed here only with the last bin shown as overflow.

### 0.3.2 FHC CC N-Tracks

This selection provides non-CCQE-like samples in FHC mode inputs to BANFF. The reconstructed momentum and angular distributions are shown in Figure 8 on page 14. Since this selection is not optimized for any particular CC topology, there are a variety of interactions modes present including 1, multiple pion (N) and deep inelastic scattering (DIS). There are a number of mis-identified lepton candidates in the form of electrons and pions.

We can examine the efficiencies and purities differentially for the selection in Figure 9 on page 15. The true signal here is any  CC interaction except  CCQE (CC non-QE) which the CC 1-Track selection is designed to select. The efficiency is high for the higher momenta and higher angle tracks suggesting this is a high $Q^2$ selection. In addition, the purity is around ~70% in this region.

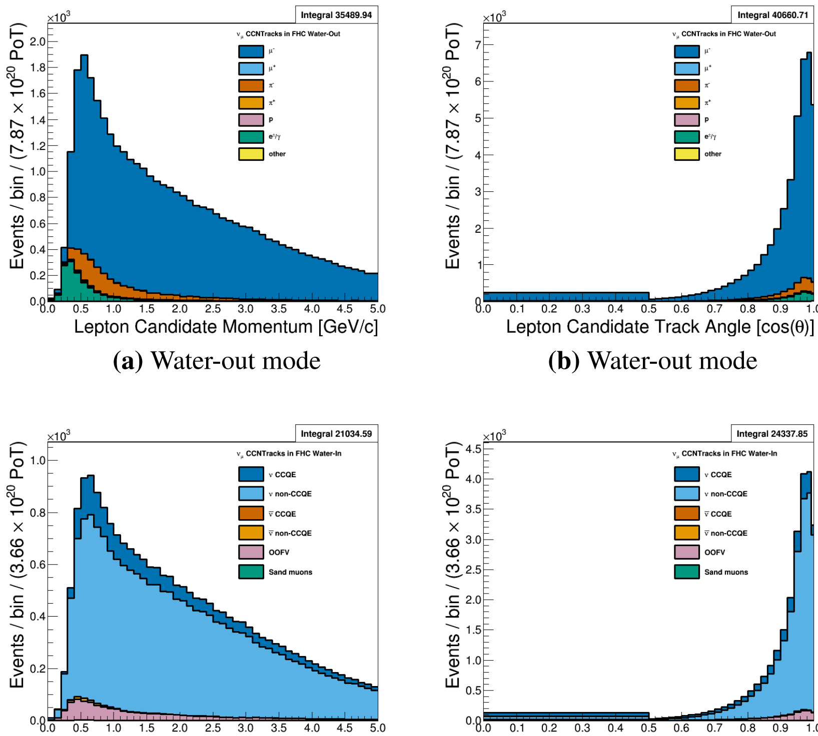


**(a)** Water-out mode **(b)** Water-out mode

**(c)** Water-in mode **(d)** Water-in mode

**Figure 8:** Lepton candidate reconstructed $P$ and $\cos\theta$ distributions for the  in FHC CC N-Tracks selection. The top figures, (a) and (b), are displaying the true neutrino interaction at the vertex and normalized to the FHC water-out mode POT. The bottom figures, (c) and (d), are displaying the true particle selected and POT normalized for the FHC water-in mode POT.

The fundamental kinematics of the selection are shown in Figure 10 on page 15. The selection captures the high energy tail of the neutrino flux which is relatively -pure. True kinematics that describe the $1$, $N$, and DIS models are parameterized in $Q^2$ and the hadronic system mass $W$. The invariant $W$ is defined as

$$W^2 = M_N^2 + 2M_N\left(E_\nu - E_l\right) - Q^2, \tag{8}$$

where $M_N$ is the mass of the struck nucleon and $E_l$ is the energy of the outgoing lepton. A dominant mode in the selection are $1$ events from a $\Delta$ resonance which has a rest mass of $1.232$ GeV/. The $\Delta$ resonance is clearly seen in the $W$ distribution in Figure 10 on page 15. Higher order resonance states are present as well since there are no cuts to distinguish minimum ionizing particles, muons and pions, from protons.

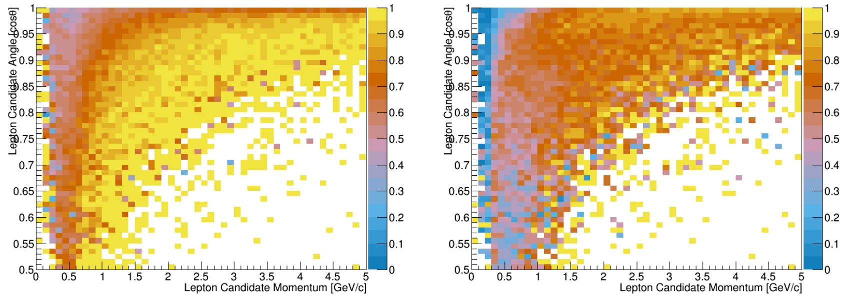


**(a)** True CC non-QE Efficiency **(b)** True CC non-QE Purity

**Figure 9:** The efficiency and purity of CC non-QE interactions in the  in FHC CC N-Tracks selection. True events are defined as correctly matched  tracks from -induced CC non-QE interactions at the vertex.

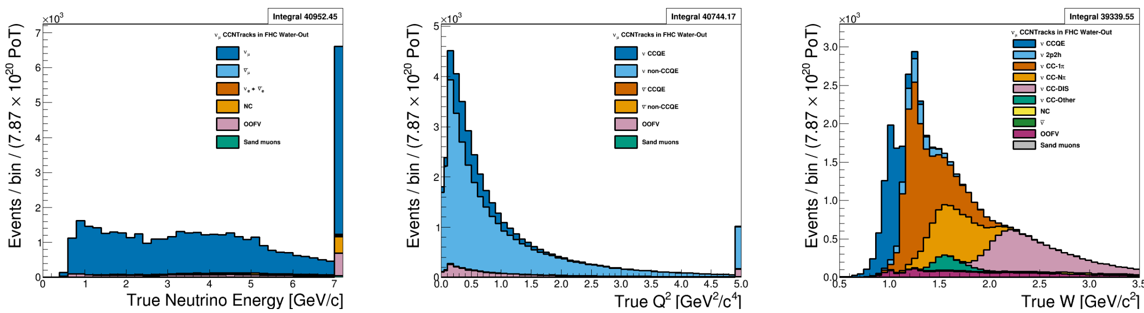


**(a)** True Neutrino Energy **(b)** True $Q^2$ **(c)** True $W$

**Figure 10:** The  in FHC CC N-Tracks true kinematics broken down by true interaction modes. Sub-figures (a), (b), and (c) show the true neutrino energy, $Q^2$, and $W$ distributions, respectively. Water-out mode is displayed here only with the last bin used as overflow is shown in (a) and (b).

The origin of the mis-identified particles, in particular the pions, becomes more clear since this is a high $Q^2$ selection. Multiple pion and DIS events can produce a negatively charged pion. For high $Q^2$ interactions topologies, the energy transfer to the final hadronic state can produce a higher energy pion than the true muon.

### 0.3.3 RHC CC 1-Track

This selection provides the  CCQE-like samples in RHC mode that are inputs to BANFF. In Figure 11 on page 16 displays the momentum and angular distributions for this selection. The selection is -pure with the selected lepton candidate being positively charged muons. There is a

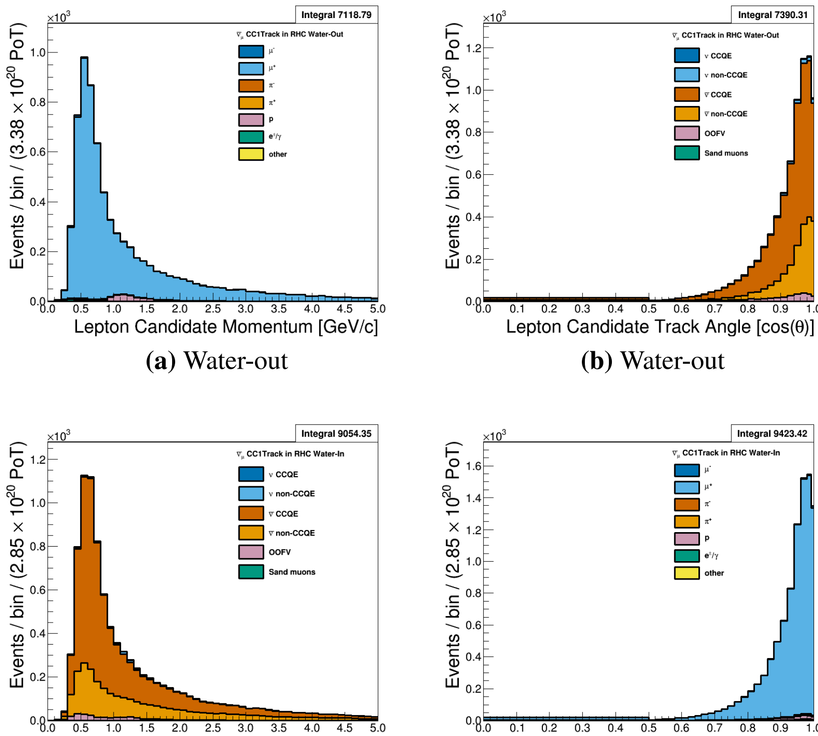


**(a)** Water-out **(b)** Water-out

**(c)** Water-in **(d)** Water-in

**Figure 11:** The  in RHC CC 1-Track $P$ and $\cos\theta$ distributions broken down by true NEUT interaction modes. The top figures (a) and (b) are water-out mode while the bottom (c) and (d) figures are water-in mode. Each distribution is normalized to the RHC POT collected between run periods 2 - 8.

large OOFV background from proton tracks. They are high momentum ($> 1$ GeV/) tracks which, at these energies, are become minimum ionizing and can reach into the TPC.

We can examine the efficiencies and purities differentially for the selection in Figure 12 on page 17, The two distributions are very similar to the  in FHC CC 1-Track efficiencies and purities, with the efficiency being relatively high (90%) for high statistics regions.

The underlying true kinematics, $E_\nu$ and $Q^2$, of the interactions are shown in Figure 13 on page 17. We see a similar true reaction composition to the  in FHC selection in Section 0.3.1. Most reactions are true CCQE with a mixture of 2p2h and $1$ events. As previously seen in Section 0.3.1, the significant $1\pi$ contamination may the BANFF reduce the sensitivity both CC $0\pi$ and CC $1\pi$ model parameters.

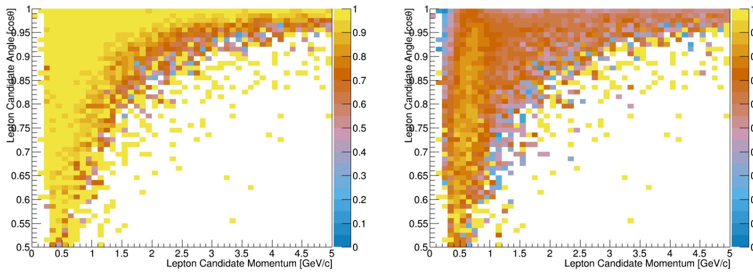


**(a)** True CCQE Efficiency **(b)** True CCQE Purity

**Figure 12:** The in RHC CC 1-Track true CCQE efficiency and purity in reconstructed kinematics. The true events are CCQE at the vertex and the selected lepton candidate is a true .

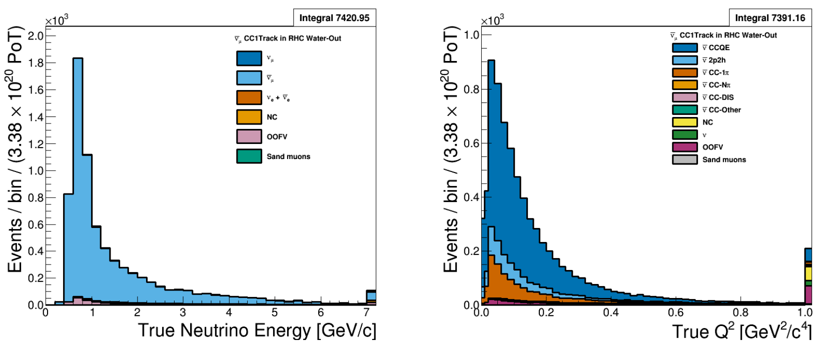


**(a)** True Neutrino Energy **(b)** True $Q^2$

**Figure 13:** The in RHC CC 1-Track true$E_\nu$ and $Q^2$ distributions. Sub-figure (a) is broken down by true neutrino flavor with (b) broken by more specific NEUT interaction modes. Water-out mode is displayed here only with the last bin used as overflow.

### 0.3.4 RHC CC N-Tracks

This selection provides the non-CCQE-like samples in RHC mode. Figure 14 on page 18 displays the momentum and angular distributions that are inputs to BANFF. The most striking feature of this selection is the the number of mis-identified events. In particular protons are selected the HMPT when they become minimum ionizing particles, which is about 1.3 GeV/c. At these energies protons can escape the () into the TPC since it deposits less energy per unit length. In addition, the intrinsic background contribution is comparable to the desired flavor. These two features should be addressed to increase the utility of the selection for the next iteration of the analysis.

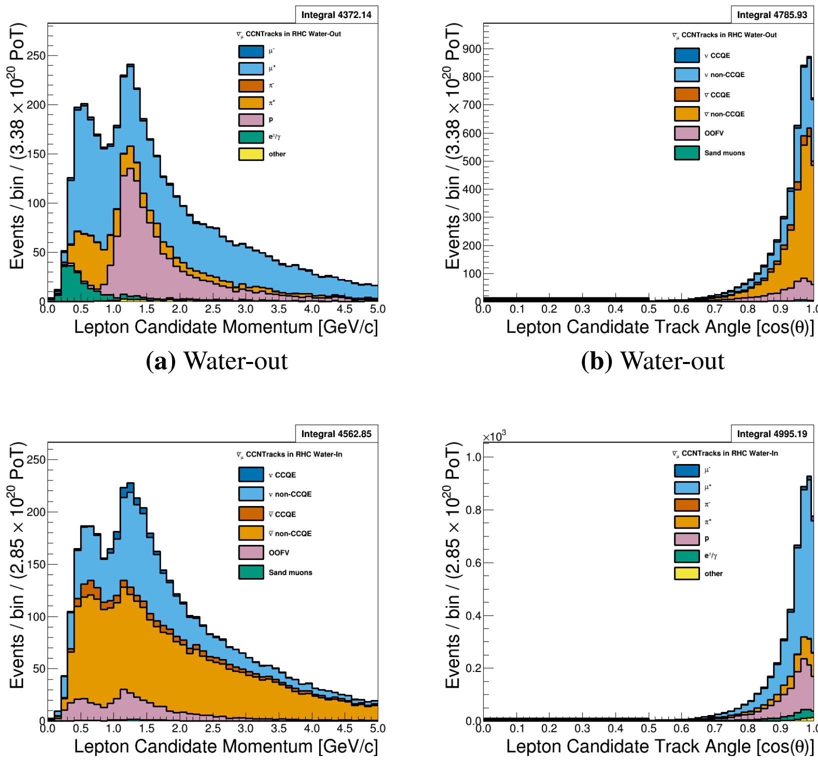


**(a)** Water-out **(b)** Water-out

**(c)** Water-in **(d)** Water-in

**Figure 14:** The  in RHC CC N-Tracks $P$ and $\cos\theta$ distributions broken down by true NEUT interaction modes. The top figures (a) and (b) are water-out mode. The bottom (c) and (d) figures are water-in mode. Each distribution is normalized to the FHC POT collected between run periods 2 - 8.

We can examine the efficiencies and purities differentially for the selection in Figure 9 on page 15. The true signal here is any  CC interaction except  CCQE which the CC 1-Track is designed to select. As seen before, both the efficiency and purity are low where statistics are relevant.

The underlying true kinematics, $E_\nu$, $Q^2$, and $W$ of the interactions are shown in Figure 16 on page 19. Here we see in better detail the origin of the  contamination. As a function of increasing energy, the  content is decreasing while the relative  contribution is increasing. The  events are also have a $Q^2$ content which explains the significant number proton main track events. For the hadronic final states, the shape of the -induced resonances is similar to what we saw in the  in FHC CC N-Tracks selections. Interestingly, the  background hadronic states are do not peak in any one region.

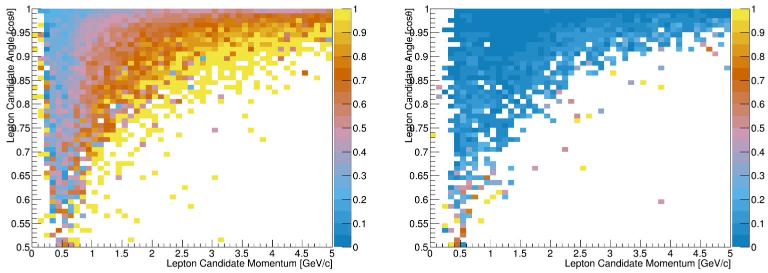


**(a)** True CC non-QE Efficiency **(b)** True non-CCQE Purity

**Figure 15:** The  in RHC CC N-Tracks true CC non-QE efficiency and purity in reconstructed kinematics. The true events are any  CC interaction except  CCQE at the vertex and the selected lepton candidate is a true .

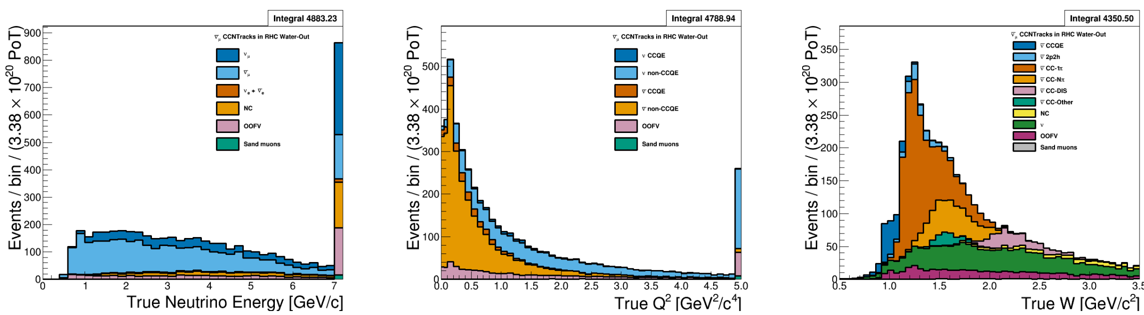


**(a)** True Neutrino Energy **(b)** True $Q^2$ **(c)** True $W$

**Figure 16:** The  in RHC CC N-Tracks $E_\nu$, $Q^2$, and $W$ distributions broken down by true NEUT interaction modes. Sub-figures (a), (b), and (c) show the true neutrino energy, $Q^2$, and $W$ distributions, respectively. Water-out mode is displayed here only with the last bin used as overflow is shown in (a) and (b).

### 0.3.5 Background in RHC CC 1-Track

This selection provides the  in RHC, also called wrong-sign background, CCQE-like samples. Figure 17 on page 20 displays the momentum and angular distributions that are inputs to BANFF. We can see this is a relatively low-angle, forward going selection compared to previous selections. Importantly the selection is -pure which should help constrain the wrong-sign background in BANFF. However, the CCQE purity is modest given number of correctly identified lepton candidates.

We can examine the efficiencies and purities differentially for the selection in Figure 18 on page 21, The efficiency is similar to the  in FHC CC 1-Track efficiency. As for the purity, it is

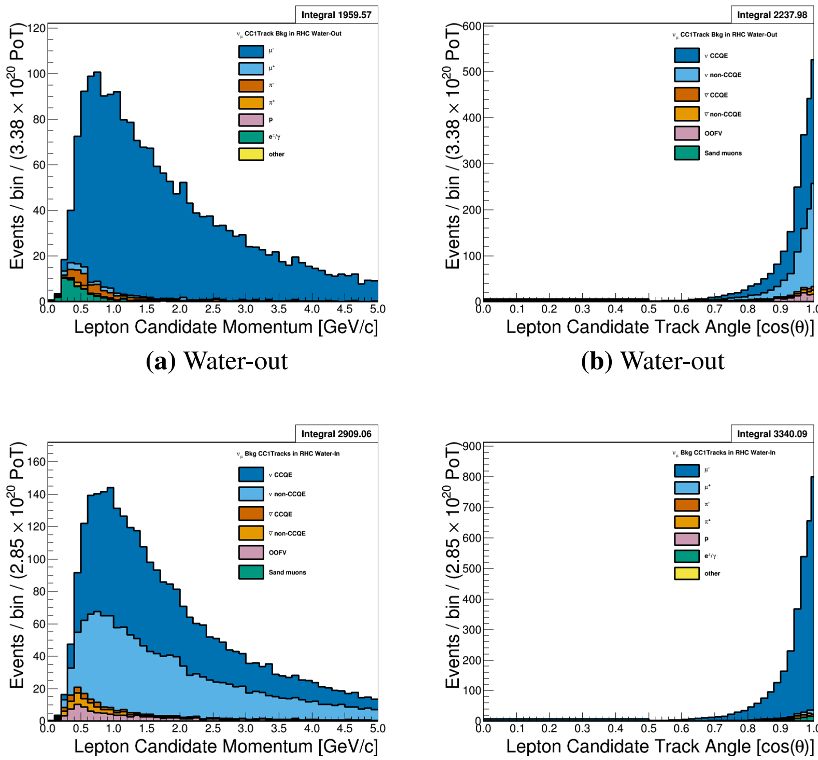


**(a)** Water-out **(b)** Water-out

**(c)** Water-in **(d)** Water-in

**Figure 17:** The  in RHC CC 1-Track $P$ and $\cos\theta$ distributions broken down by true NEUT interaction modes. The top figures (a) and (b) are water-out mode while the bottom (c) and (d) figures are water-in mode. Each distribution is normalized to the RHC POT collected between run periods 2 - 8.

roughly 70% in a banded region between low momenta, low angle and high momenta, high angle tracks.

The underlying true kinematics, $E_\nu$ and $Q^2$, of the selection are shown in Figure 19 on page 21. Due to the flux of the wrong-sign background, the neutrino energy is not sharply peaked at 0.6 GeV. This explains the significant non-CCQE event contamination in the form of 2p2h and 1 interactions.

### 0.3.6 RHC CC N-Tracks

This selection provides the  background non-CCQE-like samples in RHC mode. Figure 20 on page 22 shows the momentum and angular distributions that are inputs to BANFF. We can

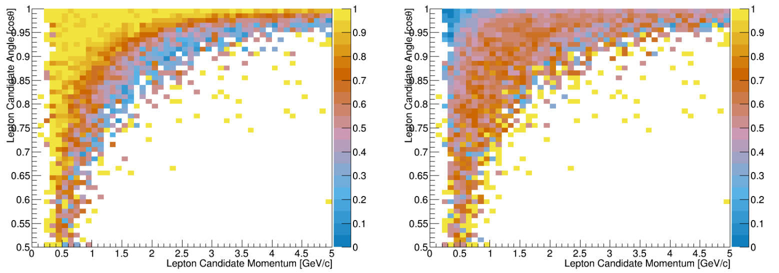


**(a)** True CCQE Efficiency **(b)** True CCQE Purity

**Figure 18:** The in RHC CC 1-Track true CCQE efficiency and purity in reconstructed kinematics. The true events are CCQE at the vertex and the selected lepton candidate is a true .

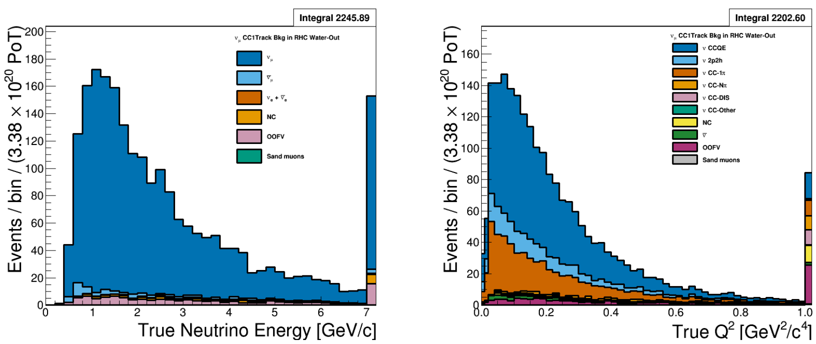


**(a)** True Neutrino Energy **(b)** True $Q^2$

**Figure 19:** The in RHC CC 1-Track true kinematic distributions broken down by true NEUT interaction modes. Sub-figure (a) is broken down by true neutrino flavor with (b) broken by more specific NEUT interaction modes. Water-out mode is displayed here only with the last bin used as overflow.

see the selection is relatively -pure with a significant mis-identified track rate. Interestingly, the mis-identified pion tracks have a high-energy trail.

We can examine the CC non-QE efficiency and purity of the selection in Figure 21 on page 23. There is a reduction in the purity below 1.5 GeV/c due to the the selections occupying the same phase space. Fortunately, the distributions are relatively high above 1.5 GeV/c.

The underlying true kinematics, $E_\nu$, $Q^2$, and $W$, of the interactions are shown in Figure 22 on page 23. As we have seen before with the CC N-Tracks samples, these are high $E_\nu$ events with large $Q^2$ exchanges. The invariant hadronic system displays the previously seen resonances, with the largest still being from the $\Delta$ baryon.

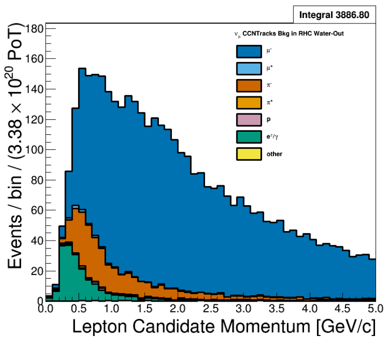


**(a)** Water-out

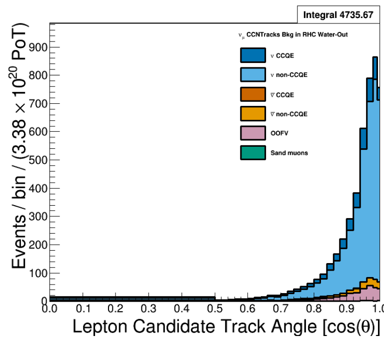


**(b)** Water-out

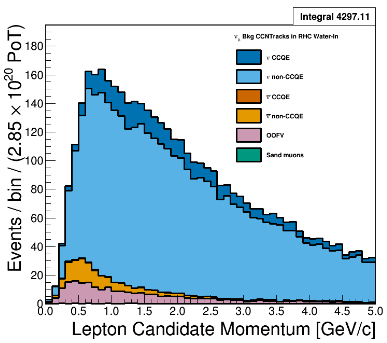


**(c)** Water-in

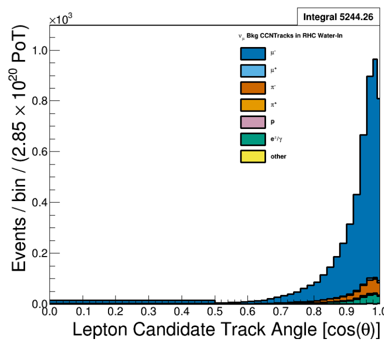


**(d)** Water-in

**Figure 20:** The  in RHC CC N-Tracks $P$ and $\cos\theta$ distributions broken down by true NEUT interaction modes. The top figures (a) and (b) are water-out mode. The bottom (c) and (d) figures are water-in mode. Each distribution is normalized to the FHC POT collected between run periods 2 - 8.

## 0.4 Summary of Selections

We have examined the selection procedure described above produces some reasonably pure CCQE samples using the 1-Track cut. By inverting that cut, we obtain some handles on other topologies like CC $1\pi$ and high $Q^2$ CCDIS events. Importantly is the ability to constrain the correct sign  and wrong sign backgrounds in RHC. We can now move forward to the systematic uncertainties present in the analysis.

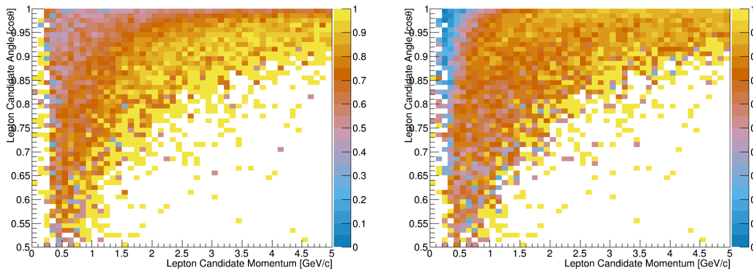


**(a)** True CC non-QE Efficiency **(b)** True non-CCQE Purity

**Figure 21:** The  in RHC CC N-Tracks true CC non-QE efficiency and purity in reconstructed kinematics. The true events are any  CC interaction except  CCQE at the vertex and the selected lepton candidate is a true .

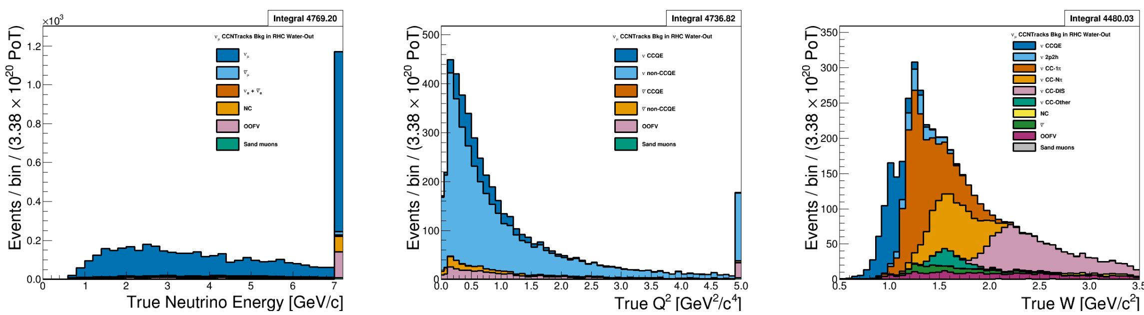


**(a)** True Neutrino Energy **(b)** True $Q^2$ **(c)** True $W$

**Figure 22:** The  in RHC CC N-Tracks true kinematics broken down by true NEUT interaction modes. Sub-figures (a), (b), and (c) show the true neutrino energy, $Q^2$, and $W$ distributions, respectively. Water-out mode is displayed here only with the last bin used as overflow is shown in (a) and (b).